Localized versus itinerant magnetic moments in $Na_{0.7}CoO_2$

J. L. Gavilano,[1] B. Pedrini,[1] K. Magishi,[2] J. Hinderer,[1] M. Weller,[1] H. R. Ott,[1] S. M. Kazakov,[1] and J. Karpinski[1]
[1]*Laboratorium für Festkörperphysik, ETH-Hönggerberg, CH-8093 Zürich, Switzerland*
[2]*Faculty of Integrated Arts and Sciences, The University of Tokushima, Tokushima 770-8502, Japan*
(Received 21 December 2005; revised manuscript received 17 May 2006; published 15 August 2006)

Based on experimental ^{59}Co-NMR data in the temperature range between 0.1 and 300 K, we address the problem of the character of the Co 3*d*-electron based magnetism in $Na_{0.7}CoO_2$. Temperature-dependent ^{59}Co-NMR spectra reveal different Co environments below 300 K and their differentiation increases with decreasing temperature. We show that the ^{23}Na- and ^{59}Co-NMR data may consistently be interpreted by assuming that below room temperature the Co 3*d* electrons are itinerant. We also argue that the ^{59}Co-NMR response is inconsistent with well-defined local magnetic moments on the Co sites. We identify a substantial orbital contribution χ^{orb} to the *d*-electron susceptibility. At low temperatures χ^{orb} seems to acquire some temperature dependence, suggesting an increasing influence of spin-orbit coupling. The temperature dependence of the spin-lattice relaxation rate $T_1^{-1}(T)$ confirms significant variations in the dynamics of this electronic subsystem between 250 and 300 K, as previously suggested. Below 100 K, $Na_{0.7}CoO_2$ may be viewed as a weak antiferromagnet with T_N below 1 K, but this scenario still leaves a number of open questions.

DOI: 10.1103/PhysRevB.74.064410 PACS number(s): 75.40.Gb, 75.20.En, 76.60.Cq, 76.60.Es

I. INTRODUCTION

During the last few years the series of layered transition-metal oxides Na_xCoO_2 with $x<1$ was the subject of intense research activities, because of the unusual electronic properties of these compounds. The variation of the Na content x revealed a rich $[T,x]$ phase diagram for this series.[1] The Na-rich region with $x>0.5$ is characterized by an unusual metallic state with a Curie-Weiss-type magnetic susceptibility χ and various trends to charge and magnetic instabilities were reported.[2–4] In particular, $\chi(T)$ suggests the presence of interacting local moments of roughly $(1-x)$ spins 1/2 per formula unit. This cannot easily be reconciled with the current understanding of the electronic structure, however. Corresponding calculations predict all the 3*d* electrons to occupy itinerant states and a relatively narrow conduction band. A very different phase is observed for $x=0.5$, which is characterized by a metal-insulator transition at 50 K (Ref. 5) and magnetic order below $T_x=88$ K.[2,6–8] Finally, the Na-poor phase $x<0.5$ exhibits the characteristics of a common metal with a Pauli-type susceptibility.

The properties of Na_xCoO_2, with $x\approx 0.7$ were extensively investigated before but a clear understanding of its physical properties is still lacking.[9–18] The Co ions are enclosed in edge sharing O-octahedra which in turn are separated by insulating Na layers.[19,20] The latter mainly act as a charge reservoir. Depending on x, the Na ions tend to order on particular sublattices at room temperature and below.[21] Considering existing experimental data, it seems difficult to describe the transport and the magnetic properties in a self-consistent manner. In particular, the postulated[22–24] itinerant 3*d*-electron system seems at odds with the claims of previous ^{23}Na-NMR studies, which reported that between 40 and 250 K the ^{23}Na-NMR response can be understood by assuming the presence of localized 3*d* moments below room temperature.[9,14] This seemed justified from observing that the Knight shifts (Ref. 25) ^{23}K of the NMR signals from different Na sites scale with the magnetic susceptibility $\chi(T)$. The latter exhibits a clear Curie-Weiss-type behavior and, in the same temperature range, the spin-lattice relaxation rate T_1^{-1} is roughly T independent. Confronted with this inconsistency we decided to revisit the problem with the analysis of an extensive set of additional experimental data.

We present the results of ^{59}Co-NMR measurements on polycrystalline samples of $Na_{0.70}CoO_2$ for temperatures below 300 K and in external magnetic fields up to 8 T. In addition, we include low-temperature ^{23}Na-NMR results in our discussion. From our data we conclude that above room temperature the Co sublattice forms an electronically homogeneous system. Upon reducing the temperature, we note a drastic change in the behavior of the spin-lattice relaxation $T_1^{-1}(T)$ for both ^{23}Na (Ref. 9) and ^{59}Co nuclei between 300 to 250 K. Below 250 K we also observe a gradual differentiation of the Co site environments. The NMR lines of two of the distinct Co sites (Co1, Co2) are found to be narrow and their temperature evolution could be monitored across the entire temperature range. The appearance of a third and fourth component in the Co NMR spectra indicates that at low temperatures the 3*d*-electron system is inhomogeneous and very close to a magnetic instability.

A detailed analysis of the data reveals the dominant role of the local orbital susceptibility with respect to the ^{59}Co-NMR spectra, contrary to interpretations of similar data in previous work.[14,16,18] Both the spin and orbital parts of χ play important roles in the spin-lattice relaxation. The most significant observation is the relation between the Knight shifts $K(T)$ of the Co1 and Co2 signals and $\chi(T)$, which indicates a substantial temperature-induced variation of the hyperfine-field coupling. Below 100 K, the system may be regarded as a weak antiferromagnet with T_N at less than 1 K. Below 50 K the orbital part of the magnetic susceptibility acquires some temperature dependence, which suggests an increasing role of the spin-orbit coupling at low temperatures.

The paper is organized as follows. In Sec. II we briefly describe the experimental techniques. Experimental data,

concerning the NMR spectra and spin-lattice relaxation rates, are presented and discussed in Sec. III. The data analysis of this section assumes that the 3*d* electrons are itinerant and the implications of this assumption, together with some remaining open questions, are discussed in Sec. IV.

II. EXPERIMENTAL DETAILS

In our experiments we used standard spin-echo techniques and a phase-coherent-type pulsed spectrometer. The measurements of the NMR spectra were performed by recording the integrated NMR signal at a fixed external magnetic field and varying stepwise the frequency or, at a fixed frequency, by varying stepwise the external magnetic field. The spin-lattice relaxation rate T_1^{-1} was measured by the saturation-recovery method where first the nuclear magnetization is destroyed by applying a long comb of rf pulses and the spin-echo signal is recorded after a variable delay. The spin-spin relaxation rate T_2^{-1} was inferred from the spin-echo lifetime, measured with a rf-pulse sequence of the form $\pi/2$-τ-π with a variable delay τ.

The sample used for the present ^{59}Co-NMR experiments is the same sample that we used for our previous ^{23}Na-NMR measurements.[9] It consists of randomly oriented powder of $Na_{0.7}CoO_2$ whose preparation was previously described.[9] The powder was characterized by x-ray and neutron powder diffraction. These experiments confirmed that our material was of single phase with lattice parameters $a=2.826(1)$ and $c=10.897(4)$ Å, corresponding to a chemical composition of Na_xCoO_2 with $x=0.7\pm0.04$.[26]

III. EXPERIMENTAL RESULTS AND DATA ANALYSIS

A. The ^{59}Co-NMR spectrum

Three examples of the central parts of the ^{59}Co-NMR spectra of $Na_{0.7}CoO_2$, taken in an external field $\mu_0 H=4.001$ T at three different temperatures are displayed in Fig. 1. For the interpretation of our NMR data it must be considered that ^{59}Co nuclei ($I=7/2$) in a noncubic environment are subject to Zeeman (H_Z) and quadrupolar (H_Q) interactions. For $H_Z \gg H_Q$, which is valid in the present case, the resulting powder pattern consists of a ^{59}Co central Zeeman transition ($-1/2 \leftrightarrow +1/2$) and three pairs of extended wings, which arise from the first-order quadrupolar perturbation of the Zeeman transitions $\pm1/2 \leftrightarrow \pm3/2$, $\pm3/2 \leftrightarrow \pm5/2$, and $\pm5/2 \leftrightarrow \pm7/2$.[27,28]

The shapes of the presented spectra reveal the components of the powder pattern[28] due to two inequivalent Co sites, denoted here as Co1 and Co2, and a broad signal denoted as Co3. It may be seen that the width of the Co3 signal increases with decreasing temperature. The spectra of Co1 and Co2 include the two central ^{59}Co Zeeman transitions and the signals of the first pairs of the quadrupolar wings ($\pm1/2 \leftrightarrow \pm3/2$) W_1 and W_2 for Co1 and Co2, respectively. The central transitions, to first order unaffected by the quadrupolar perturbation, appear very prominently at the centers of the spectra. To the left and to the right, at equal distances from the central transitions, are the maxima W_1 and W_2 of the wings. By comparing the NMR intensities, we conclude

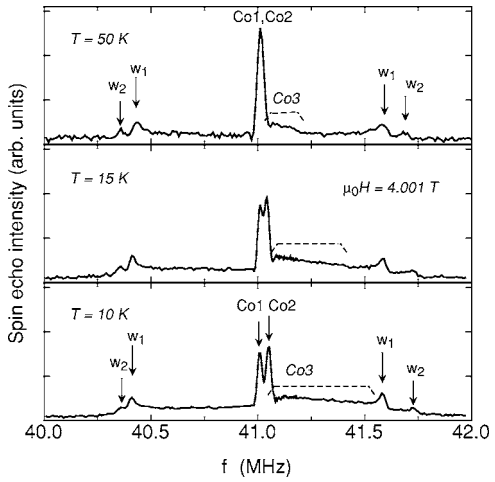

FIG. 1. ^{59}Co-NMR spectra of $Na_{0.70}CoO_2$ measured in the fixed external magnetic field of 4.001 T at three different temperatures. Two narrow signals indicate two different Co sites (Co1 and Co2) and a broad signal Co_3, accounting for a third inequivalent site, is observed on the high frequency side.

that these sites are approximately equally occupied at low temperatures. The corresponding quadrupolar frequencies, $\nu_{Q,1}$ and $\nu_{Q,2}$, i.e., the frequency difference between the maxima of the first pairs of wings at W_1 and at W_2, respectively, indicate different electric field gradients *eq* at Co1 and Co2. Most likely these sites are microscopically distributed within a single phase. If these signals originated in separated regions of macroscopic size, the equality of their NMR intensities would imply a macroscopic segregation of two different phases with volume fractions of the order of 50%, not compatible with the above-mentioned results of the structural characterization of our material using x rays and neutron scattering techniques. At lower temperatures (see lower part of Fig. 1) the positions of the central transitions gradually separate in frequency without an indication for a phase transition, however. The individual Co1 and Co2 lines of our spectra do not split at very low temperatures, i.e., below 50 K. From the temperature evolution of the central lines and of the corresponding wings it is clear that the entire spectrum of the Co1 sites shifts to lower frequencies whereas the spectrum corresponding to Co2 shifts to higher frequencies. The complete data set provides no evidence for a lowering of the point symmetry at the local Co environments between 50 K and temperatures of the order of 0.1 K. A spectrum component Co3, observed only at temperatures near 50 K and below and, as we shall see later, also an additional component Co4, seem to behave qualitatively different from Co1 and Co2. Since our data do not allow for an in-depth analysis of these parts of the spectra, their significance will only briefly be considered at the end of the discussion section.

Observations of different Co sites have previously been reported for Na_xCoO_2.[14,16,18] In general, the qualitative features of the presented ^{23}Na- and ^{59}Co-NMR spectra for $x \approx 0.7$ are rather similar to ours but the denotations are different. For example, the broad signals with large shifts and small T_2 are denoted as Co3 and Co4 in our case, but as Co2

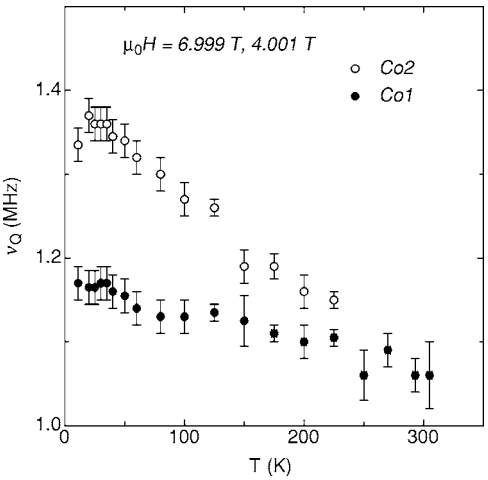

FIG. 2. Temperature dependences of the quadrupolar frequencies ν_Q of the two inequivalent Co sites Co1 and Co2. The resulting data were extracted from spectra measured at 4.001 and 6.999 T. Within experimental uncertainty they cannot be distinguished.

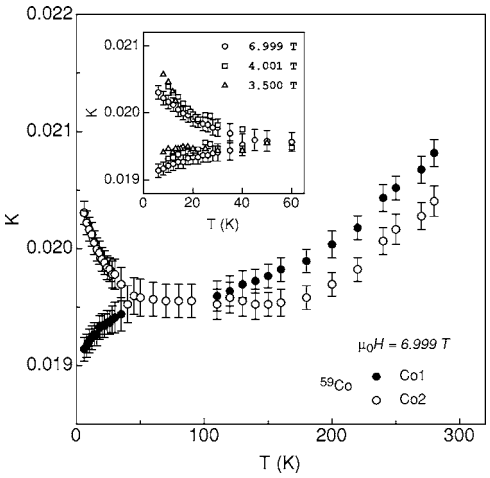

FIG. 3. Temperature dependences of the ^{59}Co Knight shifts ^{59}K. At low temperatures the behavior of the Co1 and Co2 signals are clearly different. Inset: ^{59}K at low temperatures measured in three different external magnetic fields. Between 40 and 100 K, the two signals virtually coincide.

and Co3 in Ref. 16, and as B and B′ in Ref. 18. The narrow signals, denoted as Co1 and Co2 in our case, are Co1a and Co1b in Ref. 16, and A′ splitting into two lines at low temperatures in Ref. 18. As one may infer from the results of Ref. 18 the fine details of the spectra are most likely very sensitive to the chemical composition of the sample material. As suggested in previous work,[17,18] we also conclude that the broad Co signals arise from the intrinsic $Na_{0.70}CoO_2$ phase.

In Fig. 2 we present the temperature evolution of ν_Q for the Co1 and Co2 sites. At room temperature $\nu_{Q,1} \approx \nu_{Q,2} \approx 1.05$ MHz, but below 250 K the difference $\Delta\nu_Q(T) = \nu_{Q,2}(T) - \nu_{Q,1}(T)$ gradually increases with decreasing temperature. Most likely the temperature-induced enhancement of $\Delta\nu_Q$ reflects both a rearrangement of the Na positions and a slight charge redistribution in the system of the 3*d* electrons near the Co ions. The total temperature-induced variation $[\nu_{Q,2}(10\ \mathrm{K}) - \nu_{Q,2}(300\ \mathrm{K})]/\nu_{Q,2}(300\ \mathrm{K})$ from 10 K up to room temperature is of the order of 30%, much larger than the few percent variations found in temperature dependences of quadrupolar frequencies for most 3*d* transition metals in regions far from electronic and structural instabilities. The ratio $\nu_{Q,1}/\nu_{Q,2}$ decreases from 1 at 300 K to 0.85 at liquid helium temperatures. In an effort to understand the role of the Na rearrangements in the observed changes in $\Delta\nu_Q(T)$ of the ^{59}Co NMR spectra, we compare $\Delta\nu_Q(T)$ with $^{23}T_2^{-1}(T)$, the spin-spin relaxation rate of the Na nuclei. Because $^{23}T_2^{-1}(T)$ depends on the dipolar coupling between the Na nuclei, it is very sensitive to changes in the relative positions of the Na ions. We recall that $^{23}T_2^{-1}(T)$ is roughly temperature independent between 40 and 200 K.[9] From the qualitative differences between $^{23}T_2^{-1}(T)$ and, e.g., $[\nu_{Q,2}(10\ \mathrm{K}) - \nu_{Q,2}(300\ \mathrm{K})]/\nu_{Q,2}(300\ \mathrm{K})$, it seems unlikely that the observed changes in the quadrupolar frequencies are entirely due to gradual changes in the Na ion positions. Sizable alterations in the electric field gradients at the nuclei, such as those observed here may, however, be due to subtle changes in the 3*d* electronic wave functions near the Co sites.

In the main frame of Fig. 3 we show the temperature-induced variation of the Knight shifts K of the ^{59}Co central transitions for Co1 and Co2. In both cases, K is of the order of 2% with, on an absolute scale, only minor variations between 4 and 300 K. The magnitude of K is a few times larger than the values found in nonmagnetic metals with conduction bands formed by 3*d* electrons, such as Sc, Ti, and V. Between 40 and 120 K the Knight shifts of the two Co sites coincide and K is, to a good approximation, temperature independent, similar to what is found for simple nonmagnetic metals. However, above 120 K and below 40 K, K varies with temperature. In the inset of Fig. 3 we emphasize the low-temperature data. We note that both sets of $K(T)$ are approximately field independent, indicating that the growing separation of the Co1 and Co2 resonances is roughly proportional to the external magnetic field and thus not caused by the onset of static internal fields. For external magnetic fields between 2.5 and 8 T no evidence for a magnetic phase transition is indicated by the evolution of the NMR spectra down to 0.1 K.

Regarding the entire temperature range, the functional dependences of $K(T)$ for both Co sites are remarkable, because they cannot be reconciled with the usual features of common paramagnetic metals, where $K(T)$ simply follows $\chi(T)$. In the mainframe of Fig. 4 we display the Knight shift K as a function of the magnetic susceptibility $\chi = M/H$ of the same sample, with the magnetization M measured in 5 T. The data sets for Co1 and Co2 emphasize the overall nonlinear relations between K and χ in both cases. Nevertheless, in two restricted temperature regions ($T > 120$ K and $T < 40$ K) one observes $\Delta K \propto \Delta\chi$, with different proportionality constants, as emphasized by the differently drawn lines for $K(\chi)$ in Fig. 4.

We analyze these regions separately. At high temperatures, the measured sets of $\chi(T)$ and $K(T)$ data are well represented by

$$\chi(T) = \chi_0 + C/(T - \theta_p) \tag{1}$$

and

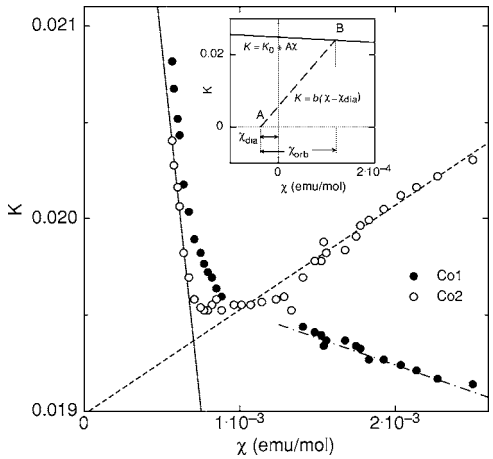

FIG. 4. $K(\chi)$ for the two sites Co1 and Co2. The solid and the broken line are, respectively, the high- and low-temperature linear fit to the data of the Co2 site. The inset shows the scheme used to extract χ^{orb} from the solid line of the main figure (see text). Note the different axes scales of the main and inset figure.

$$K = K_0 + A\chi. \tag{2}$$

From earlier work[9] we recall that $\chi_0 = 1.25 \times 10^{-4}$ (emu/mol), a rather large and positive value, $C = 0.153$ (emu K/mol) and $\theta_p = -103$ K. Values of $K_0 = K_0^{\mathrm{HT}}$ and $A = A^{\mathrm{HT}}$ obtained from fits to the $K(\chi)$ data at high temperatures (HT) are given in Table I. The low-temperature features of $\chi(T)$ deviate significantly from those captured in Eq. (1) but $K(T)$ may still be represented by Eq. (2), with distinctly different parameters $K_0 = K_0^{\mathrm{LT}}$ and $A = A^{\mathrm{LT}}$, which are listed in Table II. In spite of the Curie-Weiss-type feature in $\chi(T)$ we assume that the Co ions carry no well-defined local moment and that in a tight-binding approximation, the $3d$ electrons may be regarded as itinerant with a rather narrow conduction band.[22–24] Further we postulate the usual decompositions[28–30]

$$\chi = \chi^{\mathrm{spin}}(T) + \chi^{\mathrm{orb}} + \chi^{\mathrm{dia}} \tag{3}$$

and

$$K = K^{\mathrm{spin}}(T) + K^{\mathrm{orb}} \tag{4}$$

with

$$K^{\mathrm{spin}}(T) = (\mu_B N_A)^{-1} H_{\mathrm{hf}}^{\mathrm{cp}} \chi^{\mathrm{spin}}(T) \tag{5}$$

and

$$K^{\mathrm{orb}} = (\mu_B N_A)^{-1} H_{\mathrm{hf}}^{\mathrm{orb}} \chi^{\mathrm{orb}}. \tag{6}$$

Here the superscripts "spin" and "orb" denote the spin and the orbital contribution to χ of the $3d$ electrons, respectively. The diamagnetic part of the susceptibility χ^{dia} is due to the fully occupied atomic orbitals and is temperature independent. The shift K^{spin} is due to core polarization "cp," and the dipolar interaction of the orbital currents with the Co nuclei is responsible for K^{orb}. The total susceptibility χ is given in units of emu/mol, μ_B is the Bohr magneton, N_A is Avogadro's number and H_{hf} is the hyperfine coupling given in units of Oe per Bohr magneton of formula unit magnetization (here simply denoted as Oe). In Eq. (5) we considered the fact that for d electrons, the contact term vanishes and that, as is common for transition metals, the dipolar contribution of the electron spins is negligible.

If χ^{orb} is temperature independent, a linear $K(\chi)$ relation is obtained and, at high temperatures (HT), $K = A^{\mathrm{HT}}\chi + K_0^{\mathrm{HT}}$ with, following Eqs. (3)–(6),

$$A^{\mathrm{HT}} = (\mu_B N_A)^{-1} H_{\mathrm{hf}}^{\mathrm{cp}} \tag{7}$$

and

$$K_0^{\mathrm{HT}} = (\mu_B N_A)^{-1} [H_{\mathrm{hf}}^{\mathrm{orb}} \chi^{\mathrm{orb}} - H_{\mathrm{hf}}^{\mathrm{cp}} (\chi^{\mathrm{orb}} + \chi^{\mathrm{dia}})]. \tag{8}$$

This situation is judged to be rather common since in $3d$ metals, where the diagonal matrix elements of the angular momentum operator vanish, χ^{orb} is the analogue of the Van Vleck paramagnetism of free ions or ions in insulating crystals.[29,30]

Near electronic instabilities, $K(\chi)$ is often observed to deviate from a linear $K(\chi)$ behavior, signaling that a portion or all of χ^{orb} acquires a temperature dependence.[28] Even in this case Eqs. (3)–(6) allow K to vary linearly with χ if $\chi^{\mathrm{orb}}(T) \propto \chi^{\mathrm{spin}}(T)$. The resulting slope of $K(\chi)$ yields an effective hyperfine coupling, but the individual spin and orbital components of χ are difficult to disentangle.

With the assumption that χ^{orb} is indeed temperature independent, values of $H_{\mathrm{hf}}^{\mathrm{cp}}$ for Co1 and Co2 are obtained directly from the slopes of the lines fitting $K(\chi)$ with

$$\Delta K = [H_{\mathrm{hf}}^{\mathrm{cp}}/(N_A \mu_B)] \Delta\chi. \tag{9}$$

For $H_{\mathrm{hf}}^{\mathrm{cp}}/(10^4$ Oe) we find −4.2 and +0.3 at the Co2 site at high and low temperatures, respectively. The analogous values for the Co1 site are −4.1 and −0.15, respectively. In comparison with common transition metals and alloys these values are rather modest and confirm that the nuclei at the Co1 and Co2 sites experience rather weak hyperfine couplings to the $3d$-electron spins.[31,33]

Next we attempt an estimate of $H_{\mathrm{hf}}^{\mathrm{orb}}$ by using[32,33]

$$H_{\mathrm{hf}}^{\mathrm{orb}} = 2\mu_B \langle 1/r^3 \rangle = 12.5 \times 10^4 \langle (a_0/r)^3 \rangle \text{ (Oe)}. \tag{10}$$

A detailed knowledge of the $3d$ electronic wave function is required to evaluate $\langle (a_0/r)^3 \rangle$, which is not available at present. Fortunately it is found that $\langle (a_0/r)^3 \rangle$ does not vary much for a given transition-metal element in a variety of different environments. With $\langle (a_0/r)^3 \rangle = 6.70$ and 7.42 for Co^{3+} and Co^{4+},[31] respectively, we find $H_{\mathrm{hf}}^{\mathrm{orb}}/(10^4$ Oe$) = 83.8$ and 92.9 for Co^{3+} and Co^{4+}, respectively. Thus, regardless of the exact electronic configuration of the Co ions, $H_{\mathrm{hf}}^{\mathrm{orb}}$(Co) is expected to be an order of magnitude larger than $H_{\mathrm{hf}}^{\mathrm{cp}}$. A reasonable estimate of the average orbital hyperfine field $H_{\mathrm{hf}}^{\mathrm{orb}}(\mathrm{Co}) = 0.7 H_{\mathrm{hf}}^{\mathrm{orb}}(\mathrm{Co}^{3+}) + 0.3 H_{\mathrm{hf}}^{\mathrm{orb}}(\mathrm{Co}^{4+})$ may be justified by the content of monovalent Na ions in this compound. We thus obtain $H_{\mathrm{hf}}^{\mathrm{orb}}(\mathrm{Co})/(10^4$ Oe$) = 86.5$.

For an estimate of χ^{dia} we use the tabulated Pascal constants P in units of 10^{-6} emu/mol f.u.[34] From $0.7P_{\mathrm{Na}^{+1}} = -3.5$ for Na, $2P_{\mathrm{O}^{-2}} = -24$ for O, and $(0.7P_{\mathrm{Co}^{3+}} + 0.3P_{\mathrm{Co}^{4+}}) = -9.3$ for Co, we calculate $\chi^{\mathrm{dia}} = -0.37 \times 10^{-4}$ emu/mol f.u.

With the estimated values of $H_{\mathrm{hf}}^{\mathrm{orb}}$ and χ^{dia} we can now obtain χ^{orb} and K^{orb} via a graphical method[28,29] outlined

TABLE I. Hyperfine parameters for Co1 and Co2 at high temperatures (HT). Here $K=K_0^{\mathrm{HT}}+A^{\mathrm{HT}}\chi$, $H_{\mathrm{hf}}^{\mathrm{orb}}$ and $H_{\mathrm{hf}}^{\mathrm{cp}}$ are in units of 10^4 Oe and $\chi_0-\chi_{\mathrm{dia}}=1.62\times10^{-4}$ emu/mol.

	$K_0\times100$	A^{HT}	$H_{\mathrm{hf}}^{\mathrm{orb}}$	$H_{\mathrm{hf}}^{\mathrm{cp}}$	$\chi_{\mathrm{orb}}/(\chi_0-\chi_{\mathrm{dia}})$	$K_{\mathrm{orb}}/K_0^{\mathrm{HT}}$
Co1 HT	2.49	−7.3	86.5	−4.1	0.96	0.97
Co2 HT	2.46	−7.3	86.5	−4.1	0.95	0.97

in the inset of Fig. 4. In the $K(\chi)$ diagram we start at $(\chi=\chi^{\mathrm{dia}},K=0)$ and draw a line with the slope $b=(\mu_B N_A)^{-1}H_{\mathrm{hf}}^{\mathrm{orb}}$ (see Fig. 4). The intersection B of this line with $K(\chi)=K_0^{\mathrm{HT}}+A^{\mathrm{HT}}\chi$ from experiment and setting $\chi^{\mathrm{spin}}=0$ fixes $\chi=\chi^{\mathrm{orb}}+\chi^{\mathrm{dia}}$ and the values of χ^{orb} and K^{orb} may be extracted. At high temperatures, we obtain $\chi^{\mathrm{orb}}\approx1.55\times10^{-4}$ emu/mol and $K^{\mathrm{orb}}=0.024$ for Co2. As may be seen in Table I, similar values are obtained for Co1. It turns out that χ^{orb} is close to $\chi_0-\chi_{\mathrm{dia}}=1.62\times10^{-4}$ emu/mol and therefore, the rather large T-independent susceptibility χ_0 at high temperatures is mainly due to the orbital motion of the electrons. As presumed the Curie-Weiss-type component is thus reflecting the spin part of $\chi(T)$.

In the following we consider the low temperature region (LT), i.e., $T<40$ K. Here, the analysis is less straightforward because $\chi(T)$ deviates substantially from the Curie-Weiss behavior, observed at high temperatures. Even under the assumption that Eq. (1) still would offer a formal description of $\chi(T)$, each of the parameters χ_0, C, and θ_p would certainly be different from the values quoted above.

Quite unusual is the positive sign of $dK/d\chi=A^{\mathrm{LT}}$ observed for Co2 at LT. We recall that $H_{\mathrm{hf}}^{\mathrm{cp}}$ is almost inevitably negative, since the $1s$ and $2s$ electrons with their spins parallel to those in the tight-binding $3d$ states are attracted into the $3d$ region (outwards). This leaves a surplus of antiparallel spins at the nuclear site.[35] Therefore, the positive sign of $dK/d\chi$ clearly shows that the hyperfine coupling associated with the T-dependent part of χ cannot entirely be due to the core polarization. We interpret our $K(\chi)$ data as *prima facie* evidence for an anomalous effective hyperfine coupling, denoted here as $H_{\mathrm{hf}}^{\mathrm{eff}}$, which is not simply due to a core polarization and, in addition, is temperature independent.

As we shall discuss below, also the $T_1^{-1}(T)$ data are inconsistent with the scenario that the entire temperature variation of χ is due to χ^{spin}. We therefore consider the option that, in this temperature regime, χ^{orb} acquires some temperature dependence and $H_{\mathrm{hf}}^{\mathrm{eff}}$ reflects the combined effect of $H_{\mathrm{hf}}^{\mathrm{orb}}$ and $H_{\mathrm{hf}}^{\mathrm{cp}}$. Because K shows only a weak temperature variation and no anomalies in $T_1^{-1}(T)$ are observed below 250 K, the following analysis of $K(\chi)$ is done as before, but based on the assumptions (i) $H_{\mathrm{hf}}^{\mathrm{orb}}$ and $H_{\mathrm{hf}}^{\mathrm{cp}}$ are the same at high and low temperatures and (ii) at low temperatures only part of χ^{orb} acquires a temperature dependence, such that

$$\chi^{\mathrm{orb}}=\chi_0^{\mathrm{orb}}+\chi_1^{\mathrm{orb}}(T). \tag{11}$$

At first sight this decomposition may not seem natural. However, while all the occupied $3d$-electron states, near and far from the Fermi level, contribute to χ^{orb},[30] possible scenarios that are consistent with our observations of changes of the slopes of the linear $K(\chi)$ relations, require variations of the occupied states at or very near the Fermi surface. Only the contributions of such states to χ^{orb} would acquire a T dependence but we specify that not the entire Fermi surface needs to be involved.

For consistency, the temperature-independent term χ_1^{orb} must be small, and the desired $K(\chi)$ linear relation requests that the ratio $f=\chi_1^{\mathrm{orb}}(T)/\chi^{\mathrm{spin}}(T)$ must be temperature independent. In our particular case, one can write

$$\chi=\chi_0'+\chi'(T) \tag{12}$$

with $\chi_0'=(\chi^{\mathrm{dia}}+\chi_0^{\mathrm{orb}})$ as temperature independent and $\chi'(T)=[\chi_1^{\mathrm{orb}}(T)+\chi^{\mathrm{spin}}(T)]$. Equations (1)–(6) adapted to our case, yield the relation

$$K=K_0^{\mathrm{LT}}+(\mu_B N_A)^{-1}H_{\mathrm{hf}}^{\mathrm{eff}}\chi \tag{13}$$

with

$$H_{\mathrm{hf}}^{\mathrm{eff}}=(fH_{\mathrm{hf}}^{\mathrm{orb}}+H_{\mathrm{hf}}^{\mathrm{cp}})/(f+1)\approx fH_{\mathrm{hf}}^{\mathrm{orb}}+H_{\mathrm{hf}}^{\mathrm{cp}} \tag{14}$$

and

$$K_0^{\mathrm{LT}}=(\mu_B N_A)^{-1}[H_{\mathrm{hf}}^{\mathrm{orb}}\chi_0^{\mathrm{orb}}-H_{\mathrm{hf}}^{\mathrm{eff}}(\chi_0^{\mathrm{orb}}+\chi^{\mathrm{dia}})]. \tag{15}$$

Since $H_{\mathrm{hf}}^{\mathrm{orb}}\gg|H_{\mathrm{hf}}^{\mathrm{cp}}|\gg|H_{\mathrm{hf}}^{\mathrm{eff}}|$, $f\ll1$. Note that for $f=0$, Eqs. (7) and (8) that were used at high temperatures, are recovered.

By applying the same graphical method as before we obtained the results that are collected in Table II. Comparing the different parameters we note (i) an order of magnitude reduction of the hyperfine coupling $H_{\mathrm{hf}}^{\mathrm{cp}}$ to $H_{\mathrm{hf}}^{\mathrm{eff}}$ of the T-dependent susceptibility for both Co sites between high and low temperatures, (ii) $H_{\mathrm{hf}}^{\mathrm{eff}}$ is different in sign for the two Co sites (iii) a reduction of the low-temperature orbital susceptibility of roughly 20% with respect to the high temperature value, and (iv) the orbital parts of the susceptibility

TABLE II. Hyperfine parameters for Co1 and Co2 at low temperatures (LT). Here $K=K_0^{\mathrm{LT}}+A^{\mathrm{LT}}\chi$, $H_{\mathrm{hf}}^{\mathrm{eff}}=(fH_{\mathrm{hf}}^{\mathrm{orb}}+H_{\mathrm{hf}}^{\mathrm{cp}})$ is in units of 10^4 Oe and $\chi_0-\chi_{\mathrm{dia}}=1.62\times10^{-4}$ emu/mol.

	$K_0^{\mathrm{LT}}\times100$	A^{LT}	$H_{\mathrm{hf}}^{\mathrm{eff}}$	f	$\chi_{\mathrm{orb}}/(\chi_0-\chi_{\mathrm{dia}})$	$K_{\mathrm{orb}}/K_0^{\mathrm{LT}}$
Co1 LT	1.98	−0.28	−0.15	0.051	0.79	1.00
Co2 LT	1.90	+0.54	+0.3	0.046	0.76	1.00

dominate K_0^{HT} and K_0^{LT}. The different signs of H_{hf}^{eff} are due to small but decisive variations of the orbital component of χ.

The present analysis, based on some simplifying assumptions, suggests temperature induced changes in the 3*d* electron wave functions at low temperatures. In this scenario, a fraction of χ^{orb} adopts a substantial temperature dependence, as if part of the electrons would experience a rather strong spin-orbit coupling. The core polarization remains unchanged, but its effect on K is balanced to a high degree by modest T-induced changes in the orbital part. All this suggests that the amplitudes of 3*d*-electron wave functions vary in regions far from the Co sites, but not much near them.

Because of the nontrivial discussion of $K(\chi)$ for Co1 and Co2 we suspect that the analysis of the signals Co3 and Co4 is even more complex and may not be practical. The same procedure that we employed for estimating χ^{orb} from $K(\chi)$ (see inset of Fig. 4) is, for obvious reasons, not feasible for the signals Co3 and Co4. From our discussion above, it follows that the rather large average shifts or broad widths of Co3 and Co4 cannot simply be taken as a direct evidence for a "more magnetic" character of these sites, as would be the case if a single hyperfine mechanism, H_{hf}^{spin}, dominates. Most previous workers have assumed this to be the case,[14,16,18] but this interpretation implies a wrong sign for the spin part of the hyperfine field, i.e., a positive core polarization. By far not enough is known about these sites to allow for a reliable comparison of their magnetic properties with those of Co1 and Co2. Nevertheless, the results of our analysis outlined above suggest that it is plausible that local changes in the orbital part, rather than large changes in the spin part of the susceptibility are the main source of the observed differences in the NMR spectra of all the Co sites. In view of the character of the conduction electron band the transferred contribution to H_{hf} for Co nuclei is expected to be rather small and may therefore be neglected.

Finally we briefly compare the results of ^{59}Co-NMR with those obtained with the ^{23}Na-NMR experiments. We recall that above 40 K only a single line is observed in the ^{23}Na-NMR spectra. It corresponds to the unresolved signals of the central transitions of several, inequivalent Na sites.[9] Between 40 and 250 K, the line shift ^{23}K, representing the average isotropic signal shift at different Na sites, varies linearly with χ (see, for instance, Ihara *et al.*[15]). From $^{23}K(T)$ (unpublished results) we obtain an effective coupling of $^{23}H_{hf}=(0.83\pm0.04)\times10^4$ Oe, within the error bars of the values reported by Ihara and co-workers and also by Mukhamedshin *et al.*[15,17] This is roughly a factor of 5 smaller than H_{hf}^{cp} and of the order of 1% of H_{hf}^{orb} of ^{59}Co. At low temperatures the different Na sites are resolved in the spectra and are found to be exposed to different but also small hyperfine fields.[36] Here we simply note that (i) the hyperfine fields are consistently smaller than those at the Co sites and (ii) at all temperatures the T-independent Knight shifts for ^{23}Na are much smaller than for ^{59}Co.

B. The spin-lattice relaxation rate T_1^{-1} of ^{59}Co

In Fig. 6 we display the temperature dependence of the spin-lattice relaxation rate T_1^{-1}, measured in magnetic fields

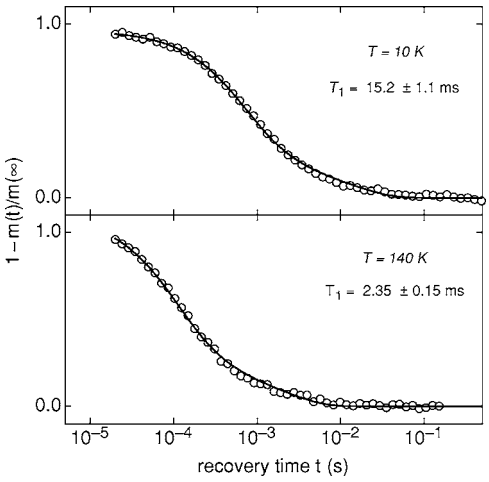

FIG. 5. Two examples of the nuclear magnetization recovery $m(t)$ data used to extract $^{59}T_1$. The data was measured at the ^{59}Co central transitions, Co1 and Co2, in an external magnetic field of 7.000 T. The solid lines represent the best fits to the data using Eq. (16).

of 4.553 and 7.045 T. The values of T_1^{-1} were extracted from fits to the nuclear magnetization recovery curves $m(t)$ of the ^{59}Co central Zeeman transition after the application of a long comb of rf pulses. In our case the appropriate fitting function for $m(t)$, assuming only magnetic relaxation, has a t-dependence of the form[37,38]

$$1-\frac{m(t)}{m_\infty}=D\left[0.41\exp\left(\frac{-28t}{T_1}\right)+0.22\exp\left(\frac{-15t}{T_1}\right)+0.18\exp\left(\frac{-6t}{T_1}\right)+0.19\exp\left(\frac{-t}{T_1}\right)\right]. \quad (16)$$

The factor D on the right-hand-side (rhs) of this equation, an additional free parameter, is an overall scaling factor to account for possible nonideal initial destruction of the nuclear magnetization. From our fits the values of D are of the order of 1 ± 0.07. Two examples of nuclear magnetization recovery data and the corresponding best fits, using Eq. (16) and thus invoking two free parameters as discussed above, are displayed in Fig. 5.

At temperatures of the order of 10 K, at which the signals from Co1 or Co2 could be irradiated individually, the possible difference in T_1^{-1} for the two sites was estimated to be of the order of 30% or less. Given the technical difficulties for a rigorous separation of the individual contributions across the entire temperature range, we neglect this difference in our analysis. The same observation applies for the ^{23}Na-NMR data, which again we describe by a single $T_1(T)$.

The features of ^{59}Co$T_1^{-1}(T)$ are clearly not those of a simple metal. Particularly prominent is the anomalous increase of $T_1^{-1}(T)$ with increasing T at $T>200$ K. A similar anomalous increase of $^{59}T_1^{-1}(T)$ seems to be indicated by the data of Ning and co-workers[18] above 200 K. An even more drastic increase was observed in $T_1^{-1}(T)$ of the ^{23}Na-NMR in the same temperature regime[9] and was associated with some kind of charge instability. Data with similar features above

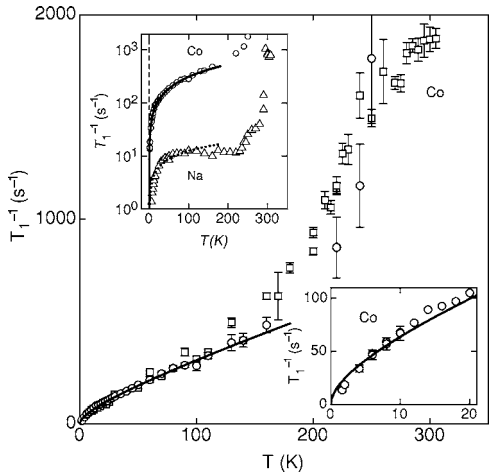

FIG. 6. Temperature dependence of the spin-lattice relaxation rate $^{59}T_1^{-1}$ measured in two different external magnetic fields and temperatures between 1.5 and 300 K. Lower inset: Details of $^{59}T_1^{-1}(T)$ at low temperatures. Upper inset: comparison of the $^{59}T_1^{-1}(T)$ and $^{23}T_1^{-1}(T)$ data. The solid and dotted lines represent fits to the data (see text).

200 K were also reported by Carreta and co-workers[14] and were interpreted as evidence for a mesoscopic phase separation in metallic and magnetic domains. In any case, the observed behavior of $T_1^{-1}(T)$ seems to be associated with the development of inhomogeneities of the Co environments below room temperature. In spite of the order of magnitude variations, the phenomenon is not really understood and the data is difficult to analyze.

In the following we concentrate on the analysis of the ^{59}Co spin-lattice relaxation data below 200 K. These data are reasonably well represented by

$$T_1^{-1} = 1.6T + 15.1\sqrt{T}, \tag{17}$$

which is illustrated by the solid lines in the main frame and the inset of Fig. 6. The first and second term are interpreted as to represent the orbital and the exchange-enhanced spin contribution, respectively.[40] In the same spirit of approximation as in Sec. III A we write

$$(T_1^{-1})^{\text{tot}} = (T_1^{-1})^{\text{orb}} + (T_1^{-1})^{\text{spin}}, \tag{18}$$

where $(T_1^{-1})^{\text{orb}}$ varies linearly with T and $(T_1^{-1})^{\text{spin}}$ represents the exchange-enhanced spin relaxation rate commonly found in nearly antiferromagnetic AF materials at $T > T_N$.[40] For such materials the staggered susceptibility $\chi_Q(T) = C_Q/(T - T_N)$ follows a Curie-Weiss-type behavior[39] and

$$(T_1^{-1})^{\text{spin}} \propto (T_1^{-1})_0^{\text{spin}} \sqrt{\chi_Q(T)} \propto T/\sqrt{(T - T_N)}. \tag{19}$$

Here $(T_1^{-1})_0^{\text{spin}} \propto T$ is the spin contribution to the relaxation rate in the absence of spin fluctuations. Our data, below 200 K and down to 1.5 K (the lowest temperature of these measurements) is well represented by assuming T_N to be less than 1 K. The low temperature data are emphasized in the lower inset of Fig. 6 and in the upper inset of the same figure we also display $T_1^{-1}(T)$ for ^{23}Na and we compare it with the data of ^{59}Co. Consistent with the very weak hyperfine interactions at the Na sites, the $^{23}T_1^{-1}(T)$ data below 100 K may be represented by a single term of the form $^{23}T_1^{-1} = 1.25\sqrt{T}$. The order of magnitude smaller prefactor, relative to the Co case, roughly reflects the squared ratio of the corresponding hyperfine couplings. The HT value of the transferred hyperfine field at the Na sites is of the order of 0.8×10^4 Oe (see the end of Sec. III A). The absence of a linear-in-T term indicates that the hyperfine field from the orbital part of the $3d$ electrons is particularly small at the Na sites, as expected for insulating Na planes.

From the first term on the rhs of Eq. (17) we may calculate the electronic density of d states at the Fermi level. The orbital contribution to the relaxation rate, appropriate for the local cubic environment of the Co sites, is given by[32,33]

$$(T_1^{-1})^{\text{orb}} = 2D'(\gamma_N H_{\text{hf}}^{\text{orb}})^2 N_{t_{2g}}(N_{t_{2g}} + 4N_{e_g})T. \tag{20}$$

The parameter $D' = (4\pi k_B \hbar)$ and the local densities of electronic states at the Fermi level (per Co atom and per spin direction) $N_{t_{2g}}$ and N_{e_g} are related to electronic states with t_{2g} and e_g symmetry, respectively. The nuclear gyromagnetic ratio γ_N is that of the Co nuclei. Previously published theoretical work claims that $N_{e_g} = 0$ for Na_xCoO_2.[22–24] With $(TT_1^{\text{orb}})^{-1} = 1.6(\text{K}^{-1}\,\text{s}^{-1})$, $H_{\text{hf}} = 86.6 \times 10^4$ Oe, and $\gamma_N = 6317$ rad/s, we obtain $N_{t_{2g}} = 1.2 \times 10^{11}$ (states/erg) per Co ion, a typical value for light d-transition metals. In the free electron approximation, this corresponds to an electronic specific heat parameter $\gamma \approx 1$ mJ mol^{-1} K^{-2}.

We emphasize that the above analysis is simplified by the fact that here, the q dependence of the hyperfine fields, which is usually difficult to estimate, plays no role since only on-site electron-nucleus interactions are relevant. The transferred hyperfine fields from neighboring Co sites are expected to be much smaller because of the predominant d character of the conduction-electron states (wave functions). Although we interpret our relaxation data differently, they are consistent with reported data from samples with the same stoichiometry. In particular our data set for $^{59}T_1(T)$ coincides, within the error bars, with that reported in Ref. 18, and our $^{23}T_1(T)$ compares very well, at least between 40 and 250 K, with that of Ihara *et al.*[15] One should keep in mind, however, that the experimental results may be very sensitive to the exact chemical composition of the investigated samples. For instance, our $^{23}T_1^{-1}(T)$ and $^{59}T_1^{-1}(T)$ data are considerably different from those for $Na_{0.75}CoO_2$, reported by Carreta and co-workers.[14]

Clearly, the temperature dependence of the spin-lattice relaxation chosen in Eq. (17) may not be unique. We simply aimed at a reasonable description of a complex system, capturing the essential features, however. The presence of ferromagnetic and antiferromagnetic correlations among the magnetic moments due to tightly bound but still itinerant Co $3d$ electrons and the very anisotropic electronic transport, with a high conductivity in the CoO_2 planes (where the correlations are of ferromagnetic type), add to the complexity. However, this may not be relevant because magnetically, the $3d$ moments are three-dimensionally coupled and, as indicated by $\chi(T)$, the antiferromagnetic interactions dominate.[9]

In closing this section we repeat that in previous work,[14,15,18] various scenarios to explain the puzzling NMR response of $Na_{0.7}CoO_2$ were discussed. We offer interpretations of the NMR spectra, that deviate from those previously published views and likewise our interpretation of the spin-lattice relaxation data is also different from those in earlier reports. While previous interpretations neglected, or played down, the role of the orbital part of the susceptibility χ^{orb} in the spin-lattice relaxation, we believe that χ^{orb} plays an essential role and hence a possible Korringa-type analysis of the spin-lattice relaxation and the Knight shift is excluded. The importance of χ^{orb} is also manifested in the occurrence of small but distinct temperature-induced changes in the NMR spectra, i.e., anomalous shifts of the Co1 and Co2 lines, with no counterpart in the corresponding spin-lattice relaxation. This puzzling observation is naturally explained in our scenario because at temperatures of the order of 40 to 100 K only a small part of χ^{orb}, acquires some temperature dependence and χ^{spin} does not change at all. Since in this temperature range the orbital and spin contributions for T_1^{-1} adopt roughly the same values, only minor changes are expected in the relaxation rate. On the other hand the NMR spectra are dominated by χ^{orb} and reflect the quoted partial change of this contribution.

Again contrary to most of the previous work, we avoid to attribute a strictly two-dimensional character to the $3d$-electron moment fluctuations. We do not find an *a priori* inconsistency between the existence of ferromagnetic correlations in the CoO planes and Moriya's theory of weak antiferromagnets.[40] Given the complex physical properties exhibited by compounds of the Na_xCoO_2 series, some guidance by improved theoretical approaches seem to be needed.

IV. DISCUSSION

In an earlier presentation[9] we concluded that the then available χ and NMR data were compatible with local-moment formation on part of the Co ions with a Co^{4+} configuration. However, the results of several calculations of the electronic structure of $Na_{0.7}CoO_2$ (Refs. 22–24) do not confirm this claim. Indeed, as discussed above, our set of ^{59}Co NMR data may be reconciled with the assumption of a set of itinerant $3d$ electrons and, as we shall see below, it is in conflict with the hypothesis of localized moments.

Below 100 K, $Na_{0.7}CoO_2$ displays features of weak antiferromagnetic metals with T_N at less than 1 K. Nevertheless some of the properties are unusual. For instance, the ^{59}Co NMR response indicates that the CoO_2 planes are electronically rather homogeneous above room temperature. Upon reducing the temperature to below 250 K, the electronic homogeneity of these planes is lost and at least four different Co environments were identified at low temperatures. As discussed before, it seems unlikely that changes in the Na-ion positions alone can account for this result. Also rather unusual are the observed variations of the hyperfine fields at the Co1 and Co2 sites. All of this suggests a temperature-induced modification of the $3d$-electron system. The increasing width of the Co3 signal with decreasing temperature suggests that as T approaches 0 K, $Na_{0.7}CoO_2$ tends to a magnetic instability.

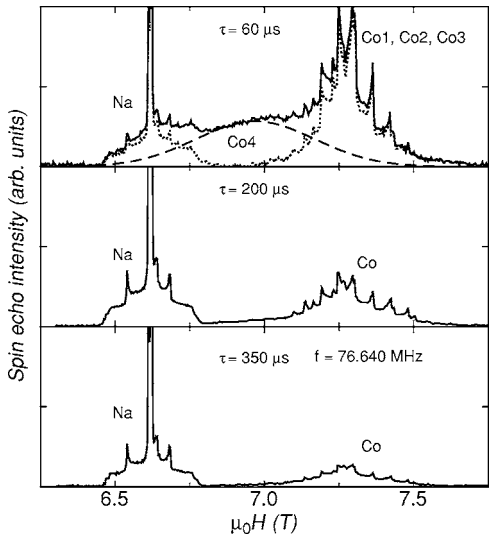

FIG. 7. ^{23}Na- and ^{59}Co-NMR spectra measured at a fixed frequency of 76.640 MHz and at a temperature of 1 K for three different pulse delays τ. Note the substantial signal near the central part of the spectrum for τ=60 μs. The broken line indicates the estimated contribution of this featureless signal (Co4), assumed to be of a Gaussian shape. The center, the amplitude and the width of this Gaussian have been adjusted so that upon its subtraction the resulting signals for the quadrupolar wings from the Na and Co1 and Co2 sites (dotted lines) are approximately symmetric.

The latter trend is best illustrated by the ^{59}Co-NMR spectra at temperatures of the order of 1 K and below. In Fig. 7 three ^{59}Co-NMR spectra recorded at fixed frequency and with three different time delays τ between the rf pulses of the spin-echo sequence are displayed. Signals with fast spin-spin relaxation can be observed for short, but not for long τ's. For a short τ=60 μs, the signal Co4, due to yet another Co environment, is observed. This signal emerges only at very low temperatures and its intensity is distributed over a very broad range of resonant fields. The related spin-spin relaxation is much faster than those of Co1 and Co2. This reveals that with decreasing T, the dynamics of the $3d$ electrons residing near the sites Co4, is slowing down dramatically and inhomogeneously, and supports the view that $Na_{0.7}CoO_2$ approaches a magnetic instability at T below 1 K, as mentioned above.

Considering our approach of postulating the d electrons as itinerant, the origin of the Curie-Weiss behavior of $\chi(T)$ should be clarified. A Curie-Weiss type $\chi(T)$ below 300 K and due to conduction electrons requires occupied electronic states in a narrow band with a width that is equivalent to a few hundred Kelvin. If we attempt a corresponding fit to our $\chi(T)$ data, the required density of electronic states $D(E_F)$ is by far larger than $D(E_F)$ resulting from our analysis of the $T_1^{-1}(T)$ data presented above. Because the effective magnetic moment p_{eff} at high temperatures is very close to the value expected from a concentration of $(1-x)$ localized, spins 1/2 in Na_xCoO_2, it is tempting to ascribe $\chi(T)$ to localized Co moments, as done before.[9] However, if one assumes such a concentration of uncompensated electronic spins to be localized or nearly localized, theoretical considerations claim that

then the material would be an insulator,[22] contrary to experimental observations.

Next we argue that the conjecture of local moments embedded in an ordinary metallic matrix leading to the Curie-Weiss-type susceptibility $\chi(T)$ is not consistent with our experimental results. Assume a concentration of $(1-x)$ spins 1/2 to be completely localized below 250 K. Hence the temperature dependence of χ arises from the corresponding localized moments and χ^{orb} and χ^{spin} due to the conduction electrons is expected to be only weakly temperature dependent. This, however, is difficult to reconcile with the presented ^{59}Co-NMR data because under these circumstances it seems impossible to account for the observed temperature-induced changes in the hyperfine fields. The scenario of postulating local moments is also confronted with the experimental observation that $\chi(T)$ not only indicates changes in their mutual interaction but also a substantial reduction of the effective moment at low temperatures. Whether these variations would influence the magnetic response of the conduction electrons such that also the hyperfine coupling issues can be explained consistently requires additional theoretical insights that are beyond the scope of this work. The same view, namely that assuming a distribution of Co^{3+} and Co^{4+} ions does not apply for $Na_{0.7}CoO_2$, was expressed in an earlier presentation[16] but was based on different arguments.

Some of the physical properties of Na_xCoO_2 seem to be rather sensitive to the Na content. For instance, most reports of the ^{59}Co-NMR spectra do not reveal an anomalous behavior of $^{59}K(T)$ below 100 K, with the possible exception of Fig. 3 of Ning and co-workers.[18] While we clearly detected the broad Co4 signal only at low temperatures, other workers reported some very broad ^{59}Co lines up to temperatures above 50 K.[16,18] At present we have no convincing explanation for this disagreement, but in part may simply be due to differences in the parameters of the detection system.

In conclusion we have shown that our NMR data, to a large extent, can be understood by assuming that the Co $3d$ electrons are itinerant and that $Na_{0.7}CoO_2$ is close to a magnetic instability at very low temperatures. Unfortunately we have no convincing arguments to explain the experimentally observed temperature dependence of the magnetic susceptibility $\chi(T)$. This and the obvious inhomogeneities of the electronic subsystem, growing with decreasing temperature, are two important issues that remain to be clarified.

ACKNOWLEDGMENTS

This work was in part financially supported by the Schweizerische Nationalfonds zur Förderung der Wissenschaftlichen Forschung (SNF). The authors have benefitted from a number of instructive discussions with M. Sigrist and M. Indergand. One of the authors (J.L.G.) thanks M. Rice and B. Batlogg for useful discussions. The study also profited from support of the NCCR program MaNEP of the SNF.

[1] M. L. Foo, Y. Wang, S. Watauchi, H. W. Zandbergen, T. He, R. J. Cava, and N. P. Ong, Phys. Rev. Lett. **92**, 247001 (2004).
[2] P. Mendels, D. Bono, J. Bobroff, G. Collin, D. Colson, N. Blanchard, H. Alloul, I. Mukhamedshin, F. Bert, A. Amato, and A. Hillier, Phys. Rev. Lett. **94**, 136403 (2005).
[3] C. Bernhard, A. V. Boris, N. N. Kovaleva, G. Khaliullin, A. V. Pimenov, Li Yu, D. P. Chen, C. T. Lin, and B. Keimer, Phys. Rev. Lett. **93**, 167003 (2004).
[4] H. W. Zandbergen, M. L. Foo, Q. Xu, V. Kumar, and R. J. Cava, Phys. Rev. B **70**, 024101 (2004).
[5] Q. Huang, M. L. Foo, J. W. Lynn, H. W. Zandbergen, G. Lawes, Y. Wang, B. H. Toby, A. P. Ramirez, N. P. Ong, and R. J. Cava, J. Phys.: Condens. Matter **16**, 5803 (2004).
[6] J. Bobroff, G. Lang, H. Alloul, N. Blanchard, and G. Collin, Phys. Rev. Lett. **96**, 107201 (2006).
[7] M. Yokoi, T. Moyoshi, Y. Kobayashi, M. Soda, Y. Yasui, M. Sato, and K. Kakurai, J. Phys. Soc. Jpn. **74**, 3046 (2005).
[8] B. Pedrini, J. L. Gavilano, S. Weyeneth, E. Felder, J. Hinderer, M. Weller, H. R. Ott, S. M. Kazakov, and J. Karpinski, Phys. Rev. B **72**, 214407 (2005).
[9] J. L. Gavilano, D. Rau, B. Pedrini, J. Hinderer, H. R. Ott, S. M. Kazakov, and J. Karpinski, Phys. Rev. B **69**, 100404(R) (2004).
[10] Y. Wang, N. S. Rogado, R. J. Cava, and N. P. Ong, Nature (London) **423**, 425 (2003).
[11] N. L. Wang, P. Zheng, D. Wu, Y. C. Ma, T. Xiang, R. Y. Jin, and D. Mandrus, Phys. Rev. Lett. **93**, 237007 (2004).
[12] M. Brühwiler, B. Batlogg, S. M. Kazakov, and J. Karpinski, cond-mat/0309311 (unpublished).
[13] B. C. Sales, R. Jin, K. A. Affholter, P. Khalifah, G. M. Veith, and D. Mandrus, Phys. Rev. B **70**, 174419 (2004).
[14] P. Carretta, M. Mariani, C. B. Azzoni, M. C. Mozzati, I. Bradaric, I. Savic, A. Feher, and J. Šebek, Phys. Rev. B **70**, 024409 (2004).
[15] Y. Ihara, K. Ishida, C. Michioka, M. Kato, K. Yoshimura, H. Sakurai, and E. Takayama-Muromachi, J. Phys. Soc. Jpn. **73**, 2963 (2004).
[16] I. R. Mukhamedshin, H. Alloul, G. Collin, and N. Blanchard, Phys. Rev. Lett. **94**, 247602 (2005).
[17] I. R. Mukhamedshin, H. Alloul, G. Collin, and N. Blanchard, Phys. Rev. Lett. **93**, 167601 (2004).
[18] F. L. Ning, T. Imai, B. W. Statt, and F. C. Chou, Phys. Rev. Lett. **93**, 237201 (2004).
[19] C. Delmas, J. J. Braconnier, C. Fouassier, and P. Hagenmuller, Solid State Ionics **3–4**, 165 (1981).
[20] R. J. Balsys and R. L. Davis, Solid State Ionics **93**, 279 (1996).
[21] Q. Huang, M. L. Foo, R. A. Pascal, Jr., J. W. Lynn, B. H. Toby, T. He, H. W. Zandbergen, and R. J. Cava, Phys. Rev. B **70**, 184110 (2004).
[22] D. J. Singh, Phys. Rev. B **68**, 020503(R) (2003).
[23] K. W. Lee, J. Kunes, and W. E. Pickett, Phys. Rev. B **70**, 045104 (2004).
[24] M. Indergand, Y. Yamashita, H. Kusunose, and M. Sigrist, Phys. Rev. B **71**, 214414 (2005).
[25] In retrospect we realize that the observed shifts of the NMR signals are, to a large extent, due to orbital contributions to the

local susceptibility. Nevertheless, here and below we denote these shifts as Knight shifts.
[26] S. M. Kazakov (private communication).
[27] A. Abragam, *Principles of Nuclear Magnetism* (Oxford University Press, New York, 1961), Chap. VII.II.A and Chap. IX.I.
[28] G. C. Carter, L. H. Bennet, and D. J. Kahan, *Metallic Shifts in NMR* (Pergamon, Oxford, 1977), Chap. VI, 6.3 and Chap. III, 3.3.
[29] V. Jaccarino, Proceedings of the International Conference on Magnetism, Nottingham, 1964, p. 377.
[30] A. M. Clogston, V. Jaccarino, and Y. Yafet, Phys. Rev. **134**, A650 (1964).
[31] A. J. Freeman and R. E. Watson, in *Magnetism*, edited by G. T. Rado and H. Suhl (Academic, New York, London, 1965), Vol. II A, p. 291.
[32] A. Narath and D. W. Alderman, Phys. Rev. **143**, 328 (1966).
[33] T. Asada, K. Terakura, and T Jarlborg, J. Phys. F: Met. Phys. **11**, 1847 (1981).
[34] E. König and G. König, *Magnetic Properties of Transition Metal Compounds*, Landolt and Börnstein, New Series II 10 (Springer, New York, 1976), Suppl. 12, pp. 12–13.
[35] R. E. Watson and A. J. Freeman, in *Hyperfine Interactions*, edited by R. J. Freeman and R. B. Frankel (Academic, New York, London, 1967), Sec. III.A, p. 59 and Sec. III.B.I.
[36] See EPAPS Document No. E-PRBMDO-74-069630 for examples of the ^{23}Na-NMR spectra at low temperatures. The data imply several inequivalent Na sites. This document can be reached via a direct link in the online article's HTML reference section or via the EPAPS homepage (http://www.aip.org/pubservs/epaps.html).
[37] A. Narath, Phys. Rev. **162**, 320 (1967).
[38] A. Suter, M. Mali, J. Roos, and D. Brinkmann, J. Phys.: Condens. Matter **10**, 5977 (1998).
[39] The variation of the uniform susceptibility is much less pronounced than that of χ_Q and it often does not display a Curie-Weiss-type behavior.
[40] T. Moriya, J. Magn. Magn. Mater. **14**, 1 (1979).